

A New Approach for Detecting Urban Centers and Their Spatial Structure With Nighttime Light Remote Sensing

Zuoqi Chen, Bailang Yu, *Senior Member, IEEE*, Wei Song, Hongxing Liu, *Member, IEEE*,
Qiusheng Wu, Kaifang Shi, and Jianping Wu

Abstract—Urban spatial structure affects many aspects of urban functions and has implications for accessibility, environmental sustainability, and public expenditures. During the urbanization process, a careful and efficient examination of the urban spatial structure is crucial. Different from the traditional approach that relies on population or employment census data, this research exploits the nighttime light (NTL) intensity of the earth surface recorded by satellite sensors. The NTL intensity is represented as a continuous mathematical surface of human activities, and the elemental features of urban structures are identified by analogy with earth’s topography. We use a topographical metaphor of a mount to identify an urban center or subcenter and the surface slope to indicate an urban land-use intensity gradient. An urban center can be defined as a continuous area with higher concentration or density of employments and human activities. We successfully identified 33 urban centers, delimited their corresponding boundaries, and determined their spatial relations for Shanghai metropolitan area, by developing a localized contour tree method. In addition, several useful properties of the urban centers have been derived, such as 9% of Shanghai administrative area has become urban centers. We believe that this method is applicable to other metropolitan regions at different spatial scales.

Manuscript received February 7, 2017; revised June 11, 2017; accepted July 4, 2017. Date of publication August 1, 2017; date of current version October 25, 2017. This work was supported in part by the National Natural Science Foundation of China under Grant 41471449, in part by the Natural Science Foundation of Shanghai under Grant 14ZR1412200, in part by the Innovation Program of Shanghai Municipal Education Commission under Grant 15ZZ026, and in part by the Fundamental Research Funds for the Central Universities of China. (*Corresponding authors:* *Bailang Yu and Jianping Wu*)

Z. Chen is with the Key Laboratory of Geographic Information Science (Ministry of Education), East China Normal University, Shanghai 200241, China, with the School of Geographic Sciences, East China Normal University, Shanghai 200241, China, and also with the Department of Geography, University of Cincinnati, Cincinnati, OH 45221 USA (e-mail: zuoqi.chen@gmail.com).

B. Yu, K. Shi, and J. Wu are with the Key Laboratory of Geographic Information Science (Ministry of Education), East China Normal University, Shanghai 200241, China, and also with the School of Geographic Sciences, East China Normal University, Shanghai 200241, China (e-mail: blyu@geo.ecnu.edu.cn; shikf1986@126.com; jpwu@geo.ecnu.edu.cn).

W. Song is with the Department of Geography and Geosciences, University of Louisville, Louisville, KY 40292 USA (e-mail: wei.song@louisville.edu).

H. Liu is with the School of Geographic Sciences, East China Normal University, Shanghai 200241, China, and also with the Department of Geography, University of Cincinnati, Cincinnati, OH 45221 USA (e-mail: Hongxing.Liu@uc.edu).

Q. Wu is with the Department of Geography, Binghamton University, State University of New York, Binghamton, NY 13902 USA (e-mail: wqs@binghamton.edu).

This paper has supplementary downloadable material available at <http://ieeexplore.ieee.org/>, provided by the author.

Color versions of one or more of the figures in this paper are available online at <http://ieeexplore.ieee.org>.

Digital Object Identifier 10.1109/TGRS.2017.2725917

Index Terms—Localized contour tree, National Polar-Orbiting Partnership-Visible Infrared Imaging Radiometer Suite (NPP-VIIRS), nighttime light (NTL) data, polycentric urban structure, topography, topological relation.

I. INTRODUCTION

URBAN structure is the spatial arrangement of land use in cities or metropolitan areas. It reflects the urban development pattern and has implications for urban functions, travel behavior, greenhouse gas emissions, loss of habitat, environmental sustainability, and public expenditures. Many theories and models have been proposed to describe and explain the urban spatial structure. Burgess [1] proposed the concentric zone model that characterizes the monocentric urban structure as five concentric rings (e.g., central business district (CBD), transition, independent workingmen’s houses, better residences, and commuters’ zone) around a single center. In recognition of spatial variation of transportation accessibility, Hoyt [2] proposed another monocentric model—the sector model. He argued that a city, as well as the actual human activity pattern, develops in sectors instead of concentric rings. Harris and Ullman [3] put forward the multiple nuclei model to describe the multinodal urban structure. According to this model, a city contains more than one center around which activities revolve. Most of these nuclei are subsidiary to the older CBD, and they can be regarded as multiple small centers at an intracity scale. Since the 1950s, urbanization in the world has evolved in such a way that relatively large urban centers with a high human activity concentration have emerged around the previous main urban center at a large metropolitan scale or at a regional scale [4], [5]. Often, these new centers are gradually developed from small towns in suburbs (also known as satellite towns or suburban downtowns) or newly spawned “edge cities” in the outlying suburbs [6], [18]. They are referred to as subcenters, which are distinguished from the traditional main center, such as CBDs [7], [8]. This new trend of polycentric urban development has been described in the literature as “dispersed city form” [9], “population and employment decentralization” [10], or “new suburbanization” [11].

Since the economic reform in 1978, many large cities in China, such as Shanghai, Beijing, and Guangzhou, have pursued a multicenter and multicorridor urban spatial structure to decentralize its population and economic activities [12]–[14]. The polycentric urban development strategy has been designed

and implemented through urban master plans, city-region plans, and urban system plans in China in order to address the transportation, housing, and environmental problems associated with densely populated monocentric cities [12], [15].

In the wake of polycentric urban growth, Liu and Wang [16] and Anas *et al.* [18] have examined the polycentric urban structure by identifying multiple subcenters and emphasizing the rising importance of suburban centers and the dynamic linkages among the central city, suburban centers, and peripheral zones of metropolitan areas. The polycentric urban structure has also been studied at greater spatial scales, including the transregional scale (e.g., the “development poles” in the European Union) and the intercity scale (e.g., the cities in the Yangzi River Delta Urban Agglomerations) [16].

An urban center, as the key element of urban spatial structure, can be defined as a continuous area characterized by higher concentration or density of employments and human activities [17]. Previous studies heavily relied on census data and local knowledge for urban center detection and urban spatial structure analysis [18], [19]. Methods in the existing literature can be classified into three groups. The first group of methods identified subcenters by setting threshold values for different census variables (e.g., employment density and population) [17], [20]–[22]. Giuliano and Small [17] defined an urban subcenter as a continuous set of adjacent transportation analysis zones that have more than 10 000 employees in the entire continuous set, and each transportation analysis zone has a minimum density of ten employees per acre.

The second group of subcenter identification methods pinpointed the local maxima in the numerical surfaces of various census variables (e.g., employment density and employment/population ratio) as urban centers or subcenters. To restrict or optimize the number of local maxima, most of such studies counted on local knowledge [23]–[26], while others adopted statistical methods, such as a locally weighted regression model [27].

The third group of methods identified urban centers through the analysis of regression residuals. McDonald and Prather [28] developed a negative exponential model to represent the employment density as a function of the distance to the CBD, and three subcenters were delimited in Chicago as a result of locating the positive residuals of the regression model. Cladura *et al.* [29] concluded that the negative exponential function is the best regression model for interpreting the spatial pattern of a polycentric urban structure after comparing a series of regression models.

Although these methods have contributed a great deal to the empirical identification of urban subcenters and urban structure, they suffer from three recurring issues. First, the census or survey data used in these methods are often collected for preset geographic units, such as census blocks or administrative regions. The shape and the extent of detected urban centers are thus limited by these preset boundaries and the way in which the areal units are defined. The interpretations about urban centers may thus be affected by the modifiable areal unit problem. Second, most of the previous methods only detected the urban centers without quantifying the properties of urban centers and the spatial and functional relationships

among them. Third, traditional methods detected the urban structure at one specific spatial scale. They were unable to construct and characterize the hierarchy of urban structure involving multiple spatial scales.

To address these issues, we employ nighttime light (NTL) data in place of census data for urban structure analysis, in which a localized contour tree method is applied to NTL data to delimit the urban centers and to analyze their spatial relationships. The NTL data record NTL intensity of the earth surface which reflects the magnitude of human activities [30]. The early generations of NTL composite data released by the National Oceanic and Atmospheric Administration’s National Geophysical Data Center (NOAA/NGDC) of the United States were acquired by the Defense Meteorological Satellite Program–Operational Linescan System (DMSP–OLS). The DMSP–OLS composite data have widely been used for delineating urban areas [31]–[33], estimating social economic indicators [34]–[39], and analyzing spatiotemporal carbon dioxide (CO_2) emission dynamics [40], [41]. However, the applications of DMSP–OLS NTL composite data have been limited due to their coarse spatial resolution (~ 1000 m), the over-saturation issue, and the lack of on-orbit calibration [42]–[45].

In early 2013, NOAA/NGDC released a new generation NTL data that are derived from the day/night band (DNB) of a new sensor—Visible Infrared Imaging Radiometer Suite (VIIRS) onboard the Suomi National Polar-orbiting Partnership (NPP) satellite. The DNB, one of the 22 bands in the VIIRS, is a calibrated panchromatic band with a wide wavelength (500–900 nm) [46]. In comparison with the DMSP–OLS NTL composite data, the NPP–VIIRS NTL composite data have a much better spatial resolution (~ 500 m) and do not suffer from NTL saturation problem owing to its wider radiometric detection range [47]–[49]. The NPP–VIIRS NTL composite data have found a wider range of applications, including estimating gross domestic product, electric power consumption, urban areas, and house vacancy rates [50]–[55].

In this paper, we present a novel method to detect urban centers based on NPP–VIIRS NTL composite data. The basic idea is to first represent the NTL intensity as topographic surface, and use light intensity contours to depict urban structure. Then, a graph-theory-based localized contour tree method [56] is applied to identify and delimit topographic mounts as urban subcenters and to determine topological relationships between adjacent urban centers.

The objectives of this paper are summarized as follows.

- 1) Conceptualize the analogy between urban spatial structure and terrain topography.
- 2) Develop an efficient method to identify the urban centers and to distinguish the main center and subcenters.
- 3) Quantitatively characterize the urban centers by several urban attributes (e.g., area, NTL density, and urban development orientation) and examine the spatial hierarchical relationships between centers.

The remainder of this paper is organized as follows. The data and study areas are described in Section II. Section III conceptualizes the analogy between urban spatial structure and topography and elaborates a methodological framework

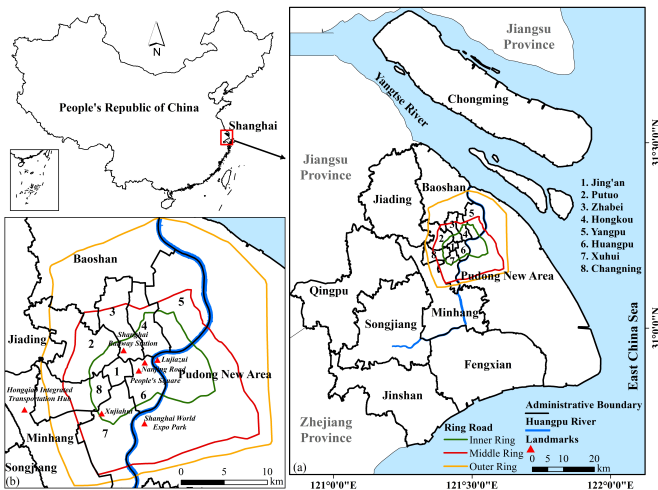


Fig. 1. (a) Geographical location of Shanghai City, China. (b) Area bounded by Outer Ring Road is enlarged to show the details.

for identifying the urban centers and depicting the urban spatial structure. In Sections IV and V, the detected urban features and corresponding urban characteristics are presented and discussed. We will summarize our findings in Section VI.

II. STUDY AREA AND DATA

A. Study Area

Our study area, Shanghai City, is among the four centrally administered municipalities in China (Fig. 1). Shanghai is located on the estuary of Yangtze River and positioned at the T-junction of two major economic belts in China, the Yangtze River basin and the East Coast. It is the leading city in China and has emerged as a global economic, financial, trade, and transportation center. The administrative municipal area of Shanghai City is as large as 6000 km², and its population is more than 23 million (the Sixth National Population Census of China, 2010). At the end of 2014, Shanghai City administers 16 districts and 1 county, including the districts of *Huangpu*, *Xuhui*, *Changning*, *Jing'an*, *Putuo*, *Zhabei*, *Hongkou*, *Yangpu*, *Minhang*, *Baoshan*, *Jiading*, *Pudong New Area*, *Jinshan*, *Songjiang*, *Qingpu*, and *Fengxian*, and *Chongming County*. The urban area inside the Outer Ring Road (yellow line in Fig. 1) is comparable to the central city (or inner city) in large western cities, enclosing an area of approximately 667.8 km². The urban area inside the Inner Ring Road (green line in Fig. 1) is the urban core of Shanghai [57], which consists of *Jing'an* and part of *Huangpu*, *Xuhui*, *Changning*, *Putuo*, *Zhabei*, *Hongkou*, *Yangpu*, and *Pudong New Area* districts. Immediately adjacent to the central city are the suburbs that include *Jiading*, *Baoshan*, *Minhang*, and part of *Pudong New Area*. Located in the city's periphery are the outlying suburbs containing *Qingpu*, *Songjiang*, *Jinshan*, and *Fengxian* districts, and *Chongming County*.

Since Chinese government adopted the economic reform and open-door policy at the end of the 1970s, Shanghai had undergone rapid social and economic development. However, the increase in the level of population, manufacturing, and production did not lead to a significant urban physical growth or the change of the city's overall urban spatial

form before 1990 [58]. The annual urban area expansion ratios were only 6 km² from 1979 to 1984 and 26.1 km² from 1984 to 1988 [59]. Consequently, the core area of central Shanghai City, including several districts on the west bank of Huangpu River (e.g., *Huangpu*, *Zhabei*, *Jing'an*, and *Hongkou* districts), experienced an intensification of land use [58], while the region of *Nanjing Road* (a famous shopping street) and the *People's Square* remained the high-density monocenter of Shanghai.

Since 1991, Shanghai has entered a new era of rapid urban transformation and development owing to the official launch of the *Pudong New Area District* development on the east bank of Huangpu River. Correspondingly, the decentralization and peripheral development have become an important strategy in the urban master plans of Shanghai City [60], [61], and the urban area has been experiencing a dramatic physical and spatial expansion. The annual urban land expansion rate from 2002 to 2008 was as high as 123.2 km² [59], which was approximately 20 times and 5 times as fast as that in 1979–1984 and in 1984–1988, respectively. Particularly, the urban spatial form has been transformed from a dense monocenter structure to an organic poly-center structure [61]–[63]. Notably, the *Lujiazui Region* in *Pudong New Area District* has been transformed from a suburban area into Shanghai's new CBD. In addition, in the Urban Development Master Plan of Shanghai (1999–2020), the “One City (Songjiang New City), Nine Towns (i.e., nine satellite towns including *Anting*, *Luodian*, *Zhujiajiao*, *Fengjing*, *Pujiang*, *Gaoqiao*, *Zhoupu*, *Fengcheng*, and *Buzhen*) Development Plan” was undertaken from 2001 to 2005 to pursue a suburban development model [60]. Later, the “One City, Nine Towns Development Plan” was replaced by the “1-9-6-6” model in 2006 as a new urban spatial structure plan for the entire administrative territory of Shanghai city. In the “1-9-6-6” model, “1” stands for the central city, “9” refers to nine new cities (*Baoshan*, *Jiading*, *Qingpu*, *Songjiang*, *Minhang*, and *Nanqiao* in *Fengxian District*, *Jinshan* and *Lingang* in *Pudong New Area District*, and *Chengqiao* in *Chongming County*), the first “6” indicates 60 small towns around nine new cities, and the second “6” indicates 600 local villages in peripheral suburban areas. Besides, the construction of several industrial parks outside the central city (such as *Zhangjiang High-Tech Industrial Park* and *Anting-Shanghai International Automobile Industrial Park*) was also initiated. Thence, Shanghai's polycentric urban structure has emerged, and this increasingly important new urban form has drawn attention from many researchers [12], [61], [62].

Four additional applications of urban centers' detection, including Beijing and Guangzhou in China, and New York and Cincinnati (located in Hamilton County, Ohio State) in the United States (Fig. S1), were also conducted in the supporting document to demonstrate how to extend the proposed urban center detection method to other world regions.

B. Data

The version 1 monthly NPP-VIIRS NTL composite data of December 2014 (http://ngdc.noaa.gov/eog/viirs/download_monthly.html, accessed August 2016) was used in this study.

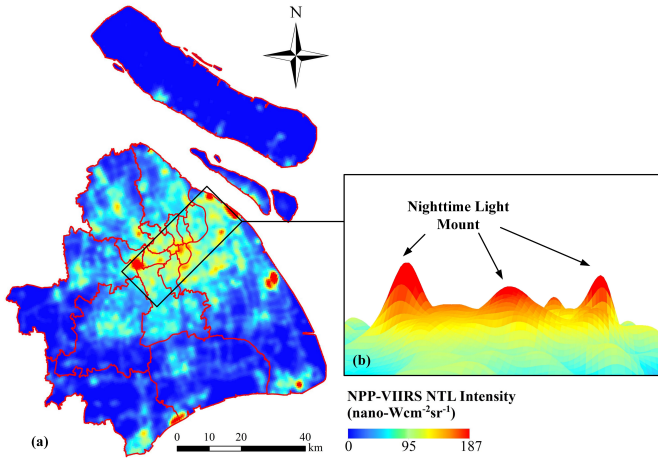


Fig. 2. (a) NPP-VIIRS NTL intensity map of Shanghai. (b) 3-D view of NTL mounts in the urban core area.

We extracted the data for Shanghai region from the global data set by using a mask polygon of Shanghai's administrative boundary with a 10-km outer buffer. The NPP-VIIRS NTL composite data were converted to the Albers Equal Area Conic projection with a pixel size of 500 m [Fig. 2(a)], and the unit of NTL intensity value is nano-Wcm⁻²sr⁻¹. The NTL intensity may be impacted by the seasonal change of vegetation [64]. Because Shanghai is in a deciduous region where many of the trees shed leaves in winter (from December to February), few trees would block the NTL beam in December. These composite data of Shanghai region were derived by averaging daily DNB data in a specific month, in which the data contaminated by the cloud cover, lunar illumination, and other factors are excluded [47], [65], [66].

The NPP-VIIRS NTL composite data used for the four additional study areas were illustrated in the supporting document, as shown in Fig. S2.

III. METHODOLOGY

A. Theoretical Basis

Functionally, the polycentric metropolitan area is normally comprised of one robust main center and a set of smaller subcenters. The urban main center and subcenters are key actors in a large polycentric metropolitan area for all aspects of urban life and activities. The main center often corresponds to the older CBD and is the focus of economic, commercial, and social activities [67]. The subcenters are subsidiary to the main center and have gradually developed from small suburb towns or newly spawned “edge cities” [18]. These urban centers have higher concentration or density of employments and human activities than surrounding areas [17]. Since the NTL intensity is positively associated with the concentration level of human activities, the NTL data for a region can be conceptualized as a continuous surface of human activity intensity, in which an urban center is a close analogy to a mount on the earth's topography. A mount manifests itself as a set of concentric contour lines in a topographic map. By analogy, the detection of an urban center can subsequently be considered as detecting an NTL mount, namely, a set of

concentric light intensity contours from the numerical surface of NPP-VIIRS NTL composite data [Fig. 2(b)].

Similarly, the surface slope, the first derivative of elevation surface, is signified by the density of contour lines [68]. The dense light intensity contour lines indicate a high spatial gradient of human activity intensity. A profile of the NTL intensity surface can reveal the spatial variation of human activity intensity and urban land-use gradient from the center to the periphery. Since the human activity and urban land-use gradients vary with the stages of urban growth, the profile and slope of NTL intensity surface may be used to depict different phases of urban growth.

Driven by the analogy between the urban structure and topography, we proposed a four-step approach to quantify the urban spatial structure based on NTL data. The first step is to generate NTL contour map from the NPP-VIIRS NTL composite data. Second, the NTL contour tree is constructed by using a localized contour tree method, and elemental urban centers are identified as leaf nodes of the contour tree. Third, we calculate a set of attributes for each urban center, including five NTL attributes, four urban morphometric attributes, and one topographical parameter. Fourth, the urban centers, as well as the hierarchical structure of urban centers, are identified to capture the spatial relationships between individual urban centers based on the simplified contour trees.

B. NPP-VIIRS NTL Contour Map Generation

In order to prevent the generated contour lines from being jagged and irregular, a three-by-three Gaussian filter with sigma of 1 was employed to smooth the NPP-VIIRS NTL composite data in order to attenuate data noise. Because the detected urban centers must be in an urban area, we first selected an NTL threshold value as the base NTL contour value in the process of generating the NTL contour map. This NTL threshold value was determined by the average NTL intensity value of the boundary of urban built-up area derived from a supervised classification of multispectral Landsat-8 image data. Five sets of training samples (built-up area samples, vegetation samples, cropland samples, barren samples, and water samples) were selected and entered into the maximum likelihood classifier to facilitate detecting and validating the urban built-up area. The classification results were then compared with hundreds of random samples, which were visually interpreted as reference data. The contour interval was set to 1 nano-Wcm⁻²sr⁻¹ for the computational efficiency in contour tree construction, and the DNB's minimum detectable radiance is approximately 0.2 nano-Wcm⁻²sr⁻¹ at nadir [69].

Since an urban center is associated with a set of concentric and closed contours, the NTL data were extracted for a larger area (a 10-km outer buffer) than study area to avoid generating open contour lines at the boundaries of the study area. In this study, the minimum urban center to be detected is defined as a center with a spatial extent of at least 5 km². Namely, if the area of a closed contour is smaller than 5 km², this contour will be dropped out without further consideration. From local knowledge, we are confident that the selection of this area threshold ensures the inclusion of all significant urban centers.

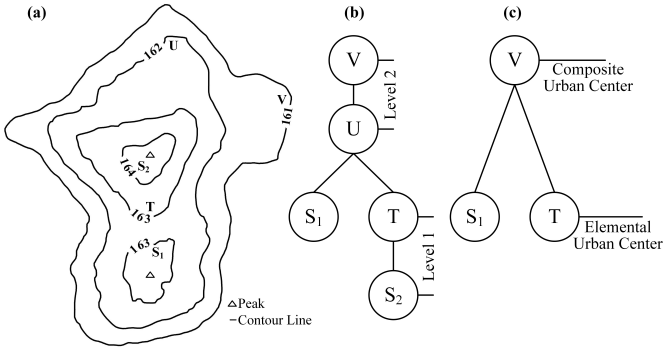


Fig. 3. Illustration of the urban center detection using the contour tree method. (a) Contour map of NTL intensity. (b) Regular contour tree. (c) Simplified contour tree.

C. Localized Contour Tree of Nighttime Light Data

The localized contour tree approach has successfully been used to identify the hierarchical structure of surface depressions from topographic data [56], [70]. This approach uses one or more graph tree(s) to quantitatively represent a contour map. A contour tree is composed of *Nodes* and *Links*. A *Node* indicates a contour line, while a *Link* represents the topological relationship between any two adjacent *Nodes* [71].

The localized contour tree generation consists of three steps [56]: locating seed contour line, generating regular localized contour tree, and simplifying contour tree. Fig. 3 illustrates how to construct a regular contour tree and a simplified contour tree based on a sample NTL intensity contour map. This sample area has two elemental urban centers (S_1 and T), which are contained in a larger composite urban center (V). An elemental urban center is the primitive urban nodal feature with a single peak on the NTL intensity surface, which is delimited by the contour of a leaf node of the simplified contour tree as explained in the following.

First, the “seed contour line” is defined as a closed contour line that does not enclose any other contour lines, but contains a local peak point [the triangle in Fig. 3(a)]. In Fig. 3, contours S_1 and S_2 are the only two seed contour lines. In a polycentric urban area, there are more than one seed contour lines. These seed contour lines are designated as level-1 nodes and treated as starting points for identifying the rank of the other contour lines in each local region. If the nearest outward contour line only contains its seed contour, this nearest outward contour line will be determined as the same level as the seed contour line. However, if a nearest outward contour line contains two or more separate branches or seed contours, this contour line will be identified as a higher level than the seed contour lines contained in it. Both nodes T and S_2 , in Fig. 3, belong to the level-1 nodes. Contour U contains contours S_1 and T , which are the two separate nodes in the regular contour tree. Thus, contour U is identified as level 2. This iterative procedure continues until all contour lines are identified and a regular contour tree is accordingly constructed [Fig. 3(b)].

The regular contour tree is then simplified to reflect the hierarchical structure of the mounts. In Fig. 3(b), contours S_2 and T belong to the same rank and constitute a branch in the contour tree graph. In a tree generated in this manner,

a branch implies no topological change inside and could be regarded as a mount. The contour of the last node represents the boundary (extent) of this mount. Therefore, only contours S_1 and T , in Fig. 3(b), are kept to represent the entire branches of S_1 and S_2-T , respectively, in the simplified contour tree. The procedure is applied to all similar branches in the contour tree, such as the branch composed of contours U and V in Fig. 3(b). V represents a composite urban center since it encloses two separate elemental urban centers at level 1. The elemental urban center is a primitive feature unit with a single nodal feature, while a composite urban center is a multinodal structure, consisting of two or more elemental urban centers.

D. Derivation of Urban Center Attributes

In the simplified NTL contour tree, the leaf nodes (level-1 nodes) are the elemental urban centers. Five statistics of the NTL value for each urban center were calculated, including minimum intensity, maximum intensity (MAX), total NTL intensity (TNTL), averaged intensity (AI), and intensity standard deviation (STD). Similarly, basic urban morphometric attributes were also computed to quantify the shape and geometric characteristics of the urban centers [33], [72]. The four urban morphometric attributes include area (S), urban development orientation (Φ), compactness index (CI), and elongatedness (ELG). CI is a shape indicator defined by the perimeter and area of an urban center [73]. In a Euclidean space, a circular object is the most compact with a CI value of 1. ELG is defined as the ratio between the length and width of the fitted minimum bounding rectangle. The definitions of above nine urban attributes are detailed in Table I.

We also calculated the slope of NTL intensity surface to reflect urban land-use intensity gradient (ULIG). For each polycentric urban system represented by a contour tree, we adopted a polycentric indicator (P) to measure the degree of polycentricity [74], [75]

$$P = 1 - \frac{\sigma_{\text{obs}}}{\sigma_{\text{max}}} \quad (1)$$

$$\sigma_{\text{obs}} = \sqrt{\frac{1}{N_c} \sum_{i=1}^{N_c} (\text{AI}_i - \bar{\text{AI}})^2} \quad (2)$$

$$\sigma_{\text{max}} = \sqrt{\frac{1}{2} ((\text{AI}_{\text{max}} - \bar{\text{AI}}_m)^2 + (0 - \bar{\text{AI}}_m)^2)} \quad (3)$$

$$\bar{\text{AI}}_m = \frac{\text{AI}_{\text{max}} + 0}{2} \quad (4)$$

where P is the degree of the morphological polycentricity of an urban area, N_c is the number of urban centers, $\bar{\text{AI}}$ and σ_{obs} are, respectively, the average value and the standard deviation of these urban centers’ AI value, and σ_{max} indicates the standard deviation of the NTL density between two urban centers—one has the highest AI value among these urban centers (AI_{max}) and the other one is a fictional center with AI of 0. The theoretical range of P is from 0 to 1. The P value of 0 indicates that this urban area is dominated by a single strong center, while the P value of 1 implies that this urban area consists of several urban centers of equal NTL intensity.

TABLE I
DEFINITIONS OF STATISTICS OF NTL VALUE AND MORPHOMETRIC CHARACTERISTICS

Attribute	Definition
Minimum Intensity (<i>MIN</i>)	$MIN = \min_{i=1}^N \{x_i\}$ N is the number of pixels in an urban center and x_i is the nighttime light intensity value of the i th pixel.
Maximum Intensity (<i>MAX</i>)	$MAX = \max_{i=1}^N \{x_i\}$
Total Nighttime Light Intensity (<i>TNTL</i>)	$TNTL = \sum_{i=1}^N x_i$
Averaged Intensity (<i>AI</i>)	$AI = TNTL / S$ S is the area of an urban center object.
Standard Deviation of Intensity (<i>STD</i>)	$STD = \sqrt{\frac{1}{N} \sum_{i=1}^N (x_i - \bar{x})^2}$ \bar{x} indicates the average nighttime light value in a contour object.
Area (<i>S</i>)	$S = N * CS$ CS is the grid cell size.
Urban Development Orientation (Φ)	An angle in degree between the x-axis and the major axis of the fitted minimum bounding rectangle. The range of orientation is from 0° to 180°
Compactness index (<i>CI</i>)	$CI = 4\pi S / P^2$ P is the perimeter of an urban center.
Elongatedness (<i>ELG</i>)	$ELG = LEN / WID$ LEN and WID are the lengths of the major and minor axis, respectively, of the fitted minimum bounding rectangle surrounding an urban center.

E. Urban Center Detection

As mentioned in Section I, Giuliano and Small [17] defined an urban center as a continuous region with an employment density and a total employment both above their respective preset cutoff values. This means that a significant and meaningful urban center should have continuous, significantly higher NTL intensity than its surrounding areas.

For a complex urbanized region, many contour trees may be identified. The “main tree” is the largest NTL contour tree in the study area, which covers the urban area with the highest NTL intensity and hence the highest concentration of human activities. Each tree represents an urban area with either monocentric or polycentric structure. For a monocentric urban structure, its contour tree has only one single branch. After the tree simplification, only one leaf node remains, and the contour line corresponding to this leaf node indicates the spatial extent of the monourban center. The contour tree of the polycentric urban structure has two or more branches. Its simplified contour tree has hence multiple leaf nodes, which represent elemental urban centers. The number of levels for a simplified contour tree reflects the complexity of the polycentric structure. The simplified contour tree in Fig. 3(c) represents a polycentric urban structure that has two elemental urban centers indicated by two leaf nodes T and S_1 . The contour lines in Fig. 3(a) corresponding to nodes T and S_1 delimit the spatial extents of urban center T and urban center S_1 . The simplified contour tree has two levels, indicating a relatively simple polycentric structure. The node V at level 2 represents a

composite urban center at a larger spatial scale, which contains two elemental urban centers T and S_1 . The spatial extent of the composite urban center V is delimited by the contour line corresponding to the contour V in Fig. 3(a).

Following Nelson [67], a city’s main center contains areas where the highest density and mix of uses in the metropolitan region occur. It exerts a strong influence over more extensive surrounding areas than a subcenter. Accordingly, we define the largest elemental center (leaf node) in the main tree as the main center and other elemental urban centers represented by other leaf nodes as urban subcenters. In Fig. 3(a), urban center T has a larger spatial extent and stronger NTL intensity and hence is identified as the main urban center, while urban center S_1 is identified as a subcenter with a weaker light intensity.

F. Uncertainty and Sensitivity Analysis

In this study, three key parameters could affect the results. The first one is the NTL threshold value, which is designed to extract the urban area and to make sure the detected urban centers are indeed in urban areas. The other two parameters are the NTL contour interval and the minimum area of the urban center. Thus, we analyzed the uncertainty and sensitivity of the results to determine the impact of these three parameters.

With the increase of the NTL threshold value, the number of detected urban centers will decrease. A range of NTL threshold values (from 30 to 36 nano-Wcm $^{-2}$ sr $^{-1}$) were selected to examine how the threshold value impacts the urban center detection, with the contour interval of 1 nano-Wcm $^{-2}$ sr $^{-1}$ and minimum urban center area of 5 km 2 . In terms of the selection of contour interval, the smaller the contour interval value, the more the accurate delineation of the urban centers and their spatial extents, but with an increased computational cost. In addition, we would not recommend using a large interval to detect urban centers because the details of detected urban centers’ location and extent would sacrifice. Therefore, four different values (0.5, 1, 1.5, and 2 nano-Wcm $^{-2}$ sr $^{-1}$) were selected to analyze how sensitive the approach is to the contour interval while using the NTL threshold value of 34 nano-Wcm $^{-2}$ sr $^{-1}$ and minimum urban center area of 5 km 2 . As for the required minimum area of the urban center, a small value could lead to detecting numerous minor urban centers or divide an intact urban center into several smaller and insignificant parts. A range of minimum area threshold values (from 0 to 7 km 2) were tested to assess their impact on the performance of urban center detection holding the NTL threshold value of 34 nano-Wcm $^{-2}$ sr $^{-1}$ and the contour interval of 1 nano-Wcm $^{-2}$ sr $^{-1}$.

IV. RESULTS

A. Elemental Urban Centers and Polycentric Structures

Based on the urban area classification via Landsat-8 image data of December 2014 with overall accuracy of 90.34% and Kappa of 0.72, the NTL contour map was generated from the NPP-VIIRS NTL composite data with the base contour value of 34 nano-Wcm $^{-2}$ sr $^{-1}$ and the contour interval of 1 nano-Wcm $^{-2}$ sr $^{-1}$ (Fig. 4). The corresponding parameters used for the four additional applications were estimated and

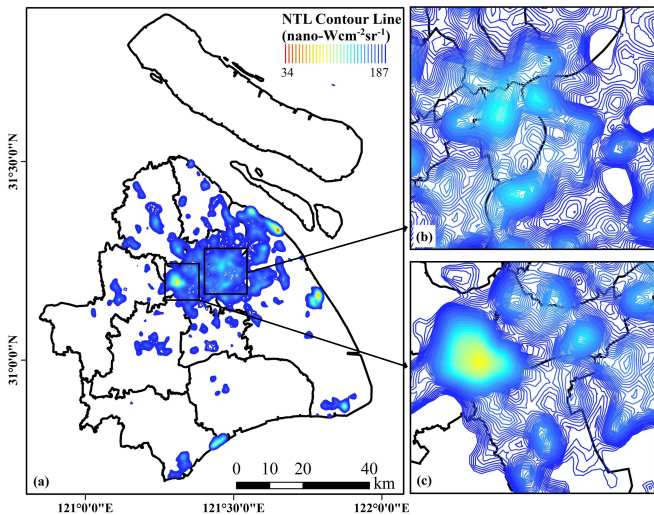


Fig. 4. (a) Contour map of Shanghai. (b) Lujiazui region and (c) Hongqiao Integrated Transportation Hub are enlarged to show the details.

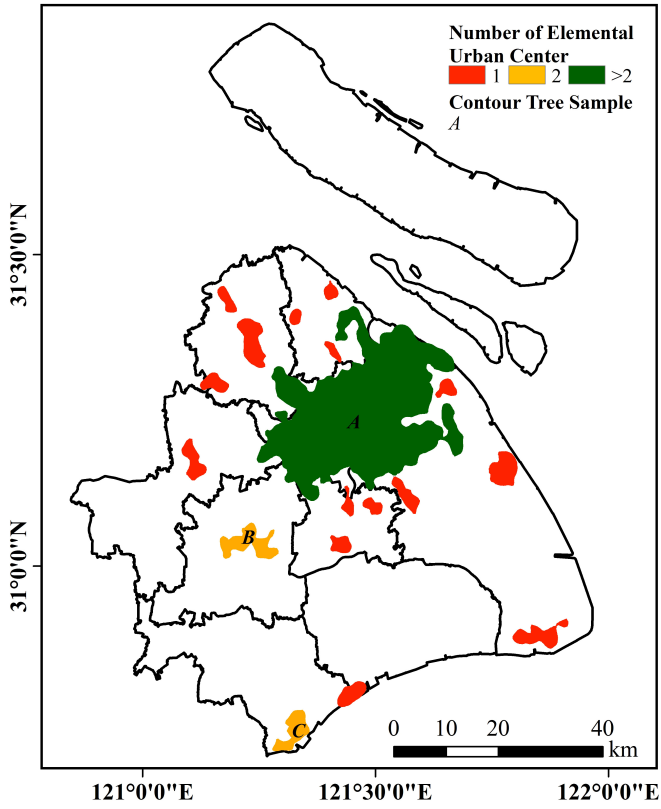


Fig. 5. Boundaries of 19 contour trees in Shanghai.

listed in Table SI in the supporting document. The color progression from red to blue in Fig. 4 symbolizes the transition in the NTL value from the highest to the lowest.

Fig. 5 depicts the spatial extents of the identified urban centers and their nested hierarchical structure in Shanghai, based on the simplified contour trees from NTL data. There are 19 contour trees derived, and these trees have 33 leaf nodes, namely, 33 elemental urban centers in total. Among these contour trees, 15 are single branch trees, indicating

a monocentric structure. Two contour trees (trees *B* and *C* in Fig. 5) have two branches (leaf nodes), and each simplified tree has two levels. One contour tree (tree *A* in Fig. 5) has more than two branches and multiple leaf nodes (see Fig. 6). The area of contour tree *A* almost occupies the entire central city (inner city) of Shanghai inside the Outer Ring Road.

Fig. 6 shows the detailed polycentric structure of tree *A*, the largest, main contour tree, in the central city area of Shanghai. Fig. 6(a) maps the contours of main tree *A*, and Fig. 6(b) shows the nested hierarchical structure of their 27 nodes with 11 hierarchical levels. Only nodes of the first five levels are discussed here to exemplify the nested hierarchical structure. The leaf nodes 1–5 represent five separate elemental urban centers. Node 15 at level 2 is considered a composite urban center because it consists of two elemental urban centers (*Node 1* and *Node 2*). Node 16 at level 3 is a broader and more complex composite urban center comprised of one elemental urban center (*Node 3*) and a composite urban center (*Node 15*) in which two elemental urban centers (*Node 1* and *Node 2*) are nested. Similarly, the polycentric urban area represented by *Node 18* at level 5 can be regarded as the most complex composite urban center in this demonstration, in which five elemental urban centers and three composite urban centers are nested at different hierarchical levels and spatial scales.

B. Validation of Detected Urban Centers

In total, 33 elemental urban centers were identified in Shanghai (Fig. 7). The main center of Shanghai is a combined area of *Lujiazui region*, *People's Square*, and *Shanghai Railway Station* (No. 1) in the main tree *A*, which has a strong NTL intensity and a homogeneous NTL distribution (low STD). Thirteen more elemental urban centers are also located in the main tree *A*, and can be considered as subcenters or multinuclei of central Shanghai City. These fourteen centers match those fourteen level-1 leaf nodes in Fig. 6. The remaining ten centers are located in the suburbs areas surrounding the central Shanghai City within 20–40 km distance to the CBD. Four centers are distributed in the outlying suburbs at a distance as far as almost 70 km from the CBD and can be considered as local centers or satellite towns. Geographical locations of these urban centers are specified in Table II. For the purpose of validation, Fig. 7 also shows the spatial distribution of the 15 reference urban centers (indicated by the red crosses in Fig. 7) which were manually identified by Sun *et al.* [12] using the local knowledge of employment density. Sun *et al.* [12] only gave the central point locations for these urban centers, without the delineation of their spatial extents. As shown in Fig. 7, all urban centers in [12] have been detected by our method with NTL data. Our method yields much more spatial details about these centers, including their spatial extent, shape, and average light intensity. One urban transportation center—*Shanghai Pudong International Airport* (No. 16)—that was missed in [12] and the urban centers in far suburban districts that were excluded in [12] have been delineated by our method, owing to the detailed information and processing efficiency of NTL data.

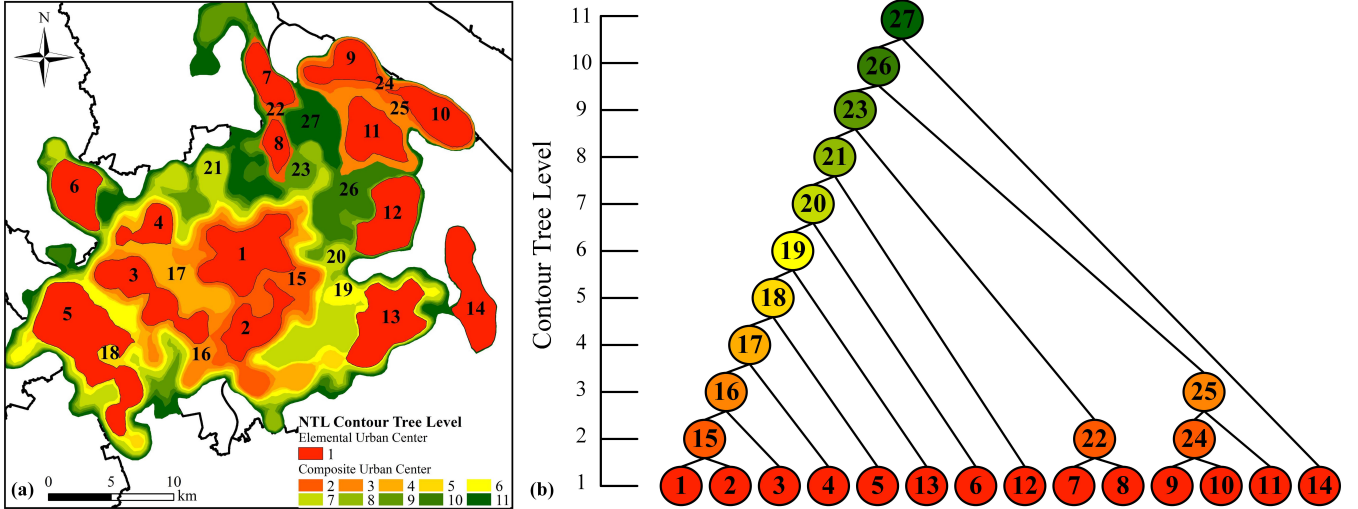


Fig. 6. (a) Contour tree of the main tree of Shanghai. (b) Nested hierarchical structure within the main tree (tree A).

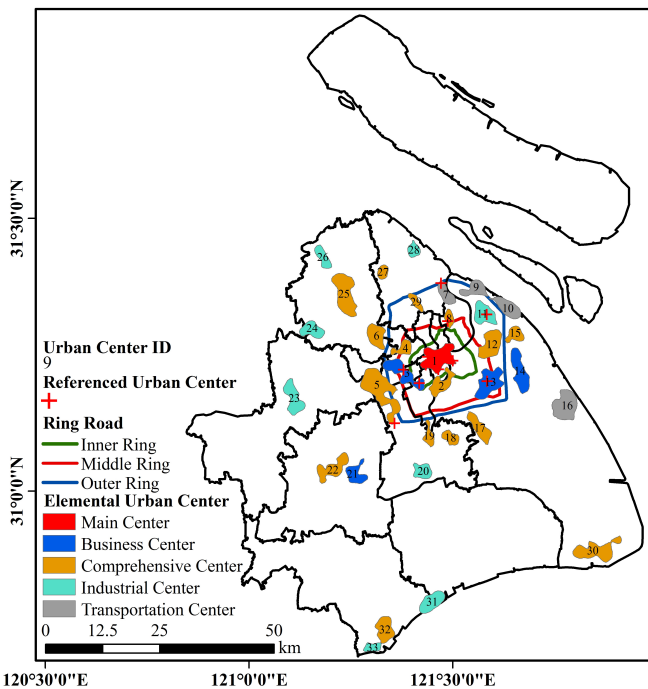


Fig. 7. Referenced urban centers and detected urban centers with primary urban function in Shanghai.

Since our approach is capable of detecting the location and spatial extent of each urban center, our analysis results can be used to evaluate the actual implementation of Shanghai's urban development plan. The "One City, Nine Towns Development Plan" and the "1-9-6-6" Plan are two crucial blueprints of urban growth for Shanghai. We compared our detected urban centers with those planned cities (towns) in Table II. The "One City" (Songjiang) and seven of the nine planned towns from the "One City, Nine Towns Development Plan," as well as seven of the nine planned new cities from the "1-9-6-6" Plan, are detected as urban centers in our study. Moreover, most of the detected urban centers that were planned in these two urban development blueprints exhibit sizable spatial extents and higher NTL intensity than other elemental urban centers. The

four planned towns or cities which were not detected as urban centers are *Fengjing* in *Jinshan District*, *Buzhen* and *Chengqiao* in *Chongming County*, and *Nanqiao* in *Fengxian District*. These planned towns or cities have not developed very well and have lower human activity density and NTL intensity in small geographical areas. Overall, our results suggest that the two urban development plans have largely been successful in implementation and in guiding Shanghai's urban restructuring and peripheral suburban growth.

Within the four additional study areas, the urban centers were also successfully detected by using this method and shown in Fig. S3.

C. Characteristics of Urban Centers

Table III displays the summary light intensity statistics and morphometric characteristics of the elemental urban centers. The average area of elemental urban centers in Shanghai is approximately 16.74 km², while the total area of all urban centers is 542 km², representing about 9% of the total land area of Shanghai's full administrative municipal territory. The TNTL and AI values vary widely, implying that the concentration level of urban activities and urban development is uneven among Shanghai's urban centers.

Fig. 8 shows the histograms of four morphometric attributes. A majority of the urban centers have an area between 5 and 20 km², while there is only one large urban center—*Hongqiao Integrated Transportation Hub* and *Xinzhuang Town* (No. 5) with a spatial extent larger than 40 km². Urban centers' CI values fall mainly from 0.50 to 0.85 [Fig. 8(c)], and most of the centers have ELG values less than 2 [Fig. 8(d)]. The combination of large CI values and small ELG values suggest that a majority of the urban centers have a relatively compact shape [e.g., *Luodian Town* (No. 27) and *Yuepu Industrial Park* (*Baoshan*) (No. 28)]. Some subcenters have followed a natural linear development pattern, which is closely related to the constraint of transportation networks or natural shorelines [76]. For instance, coastal subcenters, such as *Gaoqiaozui Port* (No. 9) and *Wuhaogou Port* (No. 10), are

TABLE II
LIST OF URBAN CENTERS IN SHANGHAI

No.	Location	Contour Tree ^a	Identified by Sun ^b	Included in "One City, Nine Towns" ^c	Included in "1-9-6-6" Plan ^d
1	Lujiazui, People's Square, Shanghai Railway Station	A	✓		△
2	Xujiahui, Shanghai World Expo Park	A			△
3	Changfeng Ecological Business District	A	✓		△
4	Zhenru	A			△
5	Hongqiao Integrated Transportation Hub, Xinzhuang Town	A	✓		○
6	Nanxiang Town	A			
7	Jungonglu Dock	A	✓		△
8	Jiangwan-Wujiaochang	A	✓		△
9	Gaoqiao Port in Waigaoqiao Port area	A		○	△
10	Wuhaogou Port in Waigaoqiao Port area	A		○	△
11	Shanghai Waigaoqiao Free Trade Zone (Gaoqiao Town)	A	✓	○	△
12	Jinqiao Town	A			△
13	Huamu, Zhangjiang Hi-Tech Park	A	✓		△
14	Shanghai Jinqiao Economic and Technological development zone	A			
15	Caolu Town	*			
16	Shanghai Pudong International Airport	*			
17	Zhoupu Town	*		○	
18	Pujiang Town	*		○	
19	Meilong Town	*			
20	Zizhu National Hi-Tech Industrial Development Zone	*			
21	Shanghai Songjiang Economic and Technological development zone	B		△	○
22	Songjiang University Town	B		△	○
23	Qingpu New Town (Zhujiajiao Town)	*		○	○
24	Anting-Shanghai International Automobile City (Anting Town)	*		○	
25	Jiading New Town	*			○
26	Shanghai Jiading Industrial Zone	*			
27	Luodian Town	*		○	
28	Yuepu Industrial Park (Baoshan)	*			○
29	Gucun Town	*			△
30	Lingang New Town	*			○
31	SINOPEC Shanghai Petrochemical Company Limited	*			
32	Jinshanwei Town	C			○
33	Shanghai Jinshan Industrial Zone	C			

a: * indicates that urban center is located in a single node contour tree. A, B and C refer to the contour tree ID in Fig. 5.

b: ✓ indicates that the urban centers are derived from Sun *et al.* (2013).

c: △ indicates the center is located in the "One City", while ○ indicates the center is included in the plan of Nine Town.

d: △ indicates the center is located in the central city ("1" in the "1-9-6-6" model), while ○ indicates the center is located in the planned new cities ("9" in the "1-9-6-6" model).

mainly oriented parallel to the coastline (indicated by an orientation angle), while the subcenters of *Zhenru* (No. 4) and *Jiangwan-Wujiaochang* (No. 8) are elongated (with a relatively large ELG) and oriented toward the main center (indicated by an orientation angle). A comparison with Shanghai Metro network reveals that the development directions of *Zhenru* (No. 4) and *Jiangwan-Wujiaochang* (No. 8) largely follow the Shanghai Metro Line 11 and Line 10, respectively.

We calculated the average light intensity slope inside each urban center to specify ULIG. As shown in Fig. 9, most urban

centers have an average slope less than 1.5%, and only ten urban centers have a steeper average slope than the overall mean (1.56%) of all urban centers. All four transportation centers, including *Jungonglu Dock* (No. 7), *Waigaoqiao Port area* (No. 9 and No. 10) and *Shanghai Pudong International Airport* (No. 16), have higher average ULIG. A comprehensive center containing a transportation hub—*Hongqiao Integrated Transportation Hub* (No. 5) also exhibits a relative high ULIG. Other three urban centers of high ULIG [*Yuepu Industrial Park* (No. 28), *Lingang New Town* (No. 30) and *SINOPEC*

TABLE III

SUMMARY STATISTICS OF URBAN CHARACTERISTICS FOR URBAN CENTERS (CI: COMPACTNESS INDEX, ELG: ELONGATEDNESS, TNTL: TOTAL NIGHTTIME LIGHT INTENSITY, AND AI: AVERAGED INTENSITY)

Statistics	Area (km ²)	CI	ELG	TNTL (nano-Wcm ⁻² sr ⁻¹)	AI (nano-Wcm ⁻² sr ⁻¹ km ⁻²)
Min	5.741	0.298	1.166	869.763	36.240
Median	15.721	0.595	1.912	3281.941	51.280
Mean	16.444	0.602	1.891	3422.116	49.239
Max	43.778	0.926	2.997	11281.529	89.546

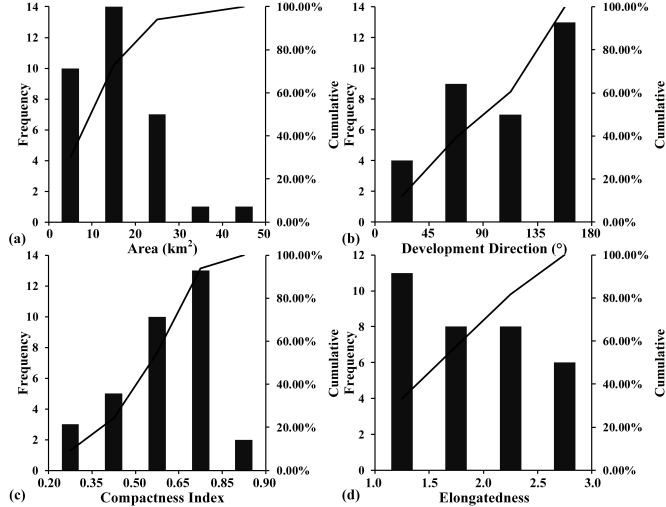


Fig. 8. Histograms of four morphometric characteristics of the urban centers: (a) Area, (b) Development Direction, (c) Compactness Index, and (d) Elongatedness.

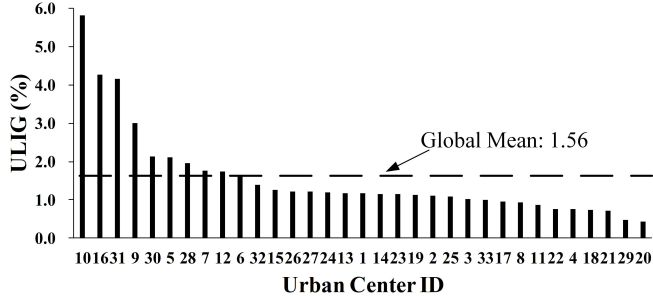


Fig. 9. Average light intensity slope (ULIG) inside the urban centers in the descending order.

Shanghai Petrochemical Company Limited (No. 31)] are all near the coast and equipped with docks.

The degree of polycentricity (P) was measured for each individual contour tree (contour trees A to C in Fig. 5) and for the entire Shanghai based on detected urban centers. The central city represented by the main tree A has a P value of 0.74, indicating a high degree of polycentricity in its structure. So it is true for the entire Shanghai City as its P value is as high as 0.73. The urban region represented by contour tree C has a high P value (0.87) since two competing urban centers nested in it are almost equally strong and neither is dominant. A similar situation exists for tree B. The contour trees of urban centers located in far suburban districts have

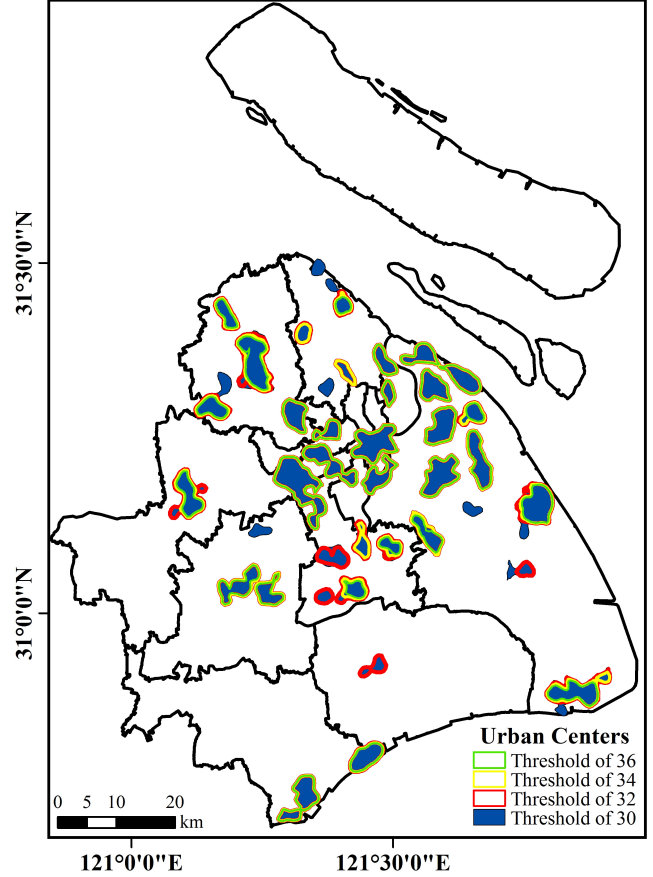


Fig. 10. Sensitivity of NTL threshold value to the urban centers' detection.

a single branch, and their urban spatial structure is typical monocentric with a P value of 0.

D. Results of Uncertainty and Sensitivity Analysis

As shown in Fig. 10, both the location and extent of urban centers inside the Outer Ring Road are not sensitive to the change in the NTL threshold values. This is partly due to the fact that the NTL values of urban centers in this region are much higher than those in the rest of Shanghai. With a low threshold value, many small urban centers outside the Outer Ring road can be detected. By comparing the urban centers detected with threshold values of 30 and 34, we found that using the threshold value of 30 can detect eight more small urban centers which are all located outside the Outer Ring Road. The average area and NTL intensity

TABLE IV
IMPACT OF CONTOUR INTERVAL ON DETECTING URBAN CENTERS

Contour Interval	Number of Urban Centers	Total Area of Urban Centers (km ²)
0.5	35	552.53
1.0	33	542.66
1.5	33	521.51
2.0	33	518.97

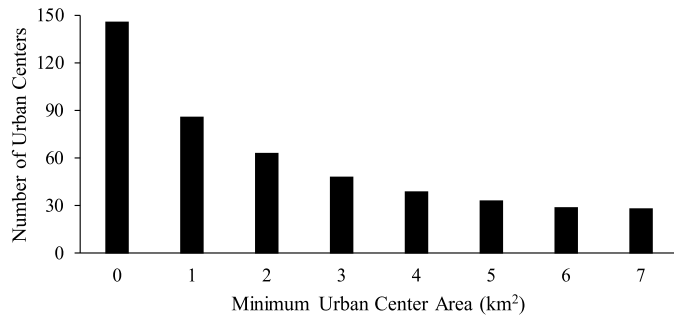


Fig. 11. Sensitivity of minimum urban center area to the urban centers' detection.

are 7 km² and 36.2 nano-Wcm⁻²sr⁻¹km⁻², which just reach the minimum level of detected urban centers' area and NTL intensity when using threshold value of 34. This sensitivity analysis indicates that the change of NTL threshold value could slightly affect the urban center detection results. Despite all this, an appropriate threshold value is still essential when using our method for detecting urban centers accurately and proper methods, such as using Landsat imagery (adopted in this study) or statistical data [77] as auxiliary data and cluster-based method [78], could be utilized to optimize the threshold value determination.

As shown in Table IV, the selection of a smaller contour interval of 0.5 leads to almost the same result as that with an interval value of 1, namely, very similar area of urban centers although two more small urban centers are detected. The urban center of *Hongqiao Integrated Transportation Hub, Xinzhuang Town* (No. 5) detected with a contour interval of 1 is split into two individual parts in the results with a contour interval of 0.5. So, in fact, only one additional urban center is detected. It is located in the *Baoshan* district and its area is only 6 km². With an interval value larger than 1, the area of urban centers slightly decreases and the number of the urban centers stays the same. We believe that our choice of a contour interval of 1 nano-Wcm⁻²sr⁻¹ is appropriate. A smaller contour interval value does not seem to improve the detection results significantly, but the computation cost could be greatly increased.

Fig. 11 illustrates that the number of detected urban centers noticeably decreases when the minimum urban center area parameter falls in the range of 0–4 km². When the parameter is greater than 4 km², the results of urban center detection become stable. This parameter is study area-specific and target driven, and in practice should be set based on the study area's spatial extent, its urbanization level, and specific application target.

V. DISCUSSION

A. Urban Spatial Structure of Shanghai City

From the NTL remote sensing data, we have derived the NTL intensity, geometric, and morphological attributes for urban centers. These characteristics may closely be related to the economic functions and land-use types of corresponding areas. According to Giuliano and Small [17], urban functions can be classified into four general categories: comprehensive service function, industrial function, transportation function, and business function. By using local knowledge, we label all detected urban centers with their primary functions in Fig. 7.

It can be seen that business centers and comprehensive centers dominate the central city area. Industrial centers, on the other hand, have been decentralized in suburbanization process at the intraurban scale. Suburbanization indicates a growing percentage of employment and economic activities in the suburban ring in comparison with the central city (inner city). Five industrial centers are located 20–40 km from the CBD in the inner suburbs, and two centers are in the outlying suburbs more than 50 km away from the city center. Planned new towns, such as *Lingang New Town* and *Jinshanwei Town*, have been developed into comprehensive subcenters in the outlying suburban. These new towns will be very likely to serve as the nucleus for the future suburban development.

Several centers are dominated by comprehensive service function, such as *Jiangwan–Wujiaochang* (No. 8) and *Zhenru* (No. 4). With further urban growth, some nearby urban centers could coalesce into a composite urban center with multiple functions. For example, the current main urban center covers the *Lujiazui* region and *the People's Square* with comprehensive service function and *Shanghai Railway station* with transportation function.

Several urban centers that we detected have a dominant function of transportation, such as *Shanghai Pudong International Airport* and *Waigaoqiao Port area*. Among seven urban centers with the highest light intensity slope, five urban centers have strong transportation function. Transportation facilities and terminals represent a special type of urban land use. Economic activities in the transport terminal areas tend to be more diverse, including transport infrastructure (e.g., airfield and terminal, rail station, and ground transportation), warehouses, industries, and services (business and consumer). This diverse mix of land uses often with strong outdoor lighting facilities, along with the separation of airports or terminals from populated land-use areas, may help explain the observed high light intensity slope in these centers.

The localized contour trees created from NTL data reveal a nested hierarchical urban structure and uncover the spatial relationships among elemental urban centers. Fig. 6(a) displays the urban structural hierarchy around the main center. The *Lujiazui*, *People's Square*, *Shanghai Railway Station* (Node 1), and *Xujiahui* and *Shanghai World Expo Park* (Node 2) were detected as two elemental urban centers at level 1 (at small spatial scale). These two urban centers have spatially and functionally integrated with each other. At a larger spatial scale (level 2), these two centers can be regarded as integral parts of a larger, composite center (a larger urban region)

delineated by the contour line of *Node 15*. This region corresponds to the innermost agglomeration and the urban heart of Shanghai, having a great concentration of modern high-rise buildings, business offices, and high-order financial and consumer services functions. At an even broader spatial scales (level 3 and level 4), *Changfeng Ecological Business District* (*Node 3*), and *Zhenru* (*Node 4*) are integrated with the main center (*Node 1*) and *Xujiahui and Shanghai World Expo Park* (*Node 2*) to form more complex polycentric urban regions (or composite centers) represented by the contours of *Node 16* and then *Node 17*. The spatial integration level of *Lujiazui, People's Square, Shanghai Railway Station* (*Node 1*), and *Xujiahui and Shanghai World Expo Park* (*Node 2*) with *Changfeng Ecological Business District* (*Node 3*) is higher than that of *Zhenru* (*Node 4*). The urban core of Shanghai can thus be considered as a spatial and functional integration of a number of nested elemental urban centers with different hierarchical orders and economic specializations. Shanghai's urban core (*Node 17*) has begun to spatially connect with the urban centers of *Hongqiao Integrated Transportation Hub* and *Xinzhuang Town* (*Node 5*), even though the connection between these two nodes is not so obvious. The spatial integration of this key transportation urban center with the urban core area is expected to increase in the future due to its high accessibility based on efficient public transit.

B. Merits and Potential Applications of Proposed Methods

In this study, the NTL measurements were treated as topography-like surface elevation data, reflecting the spatial variation of the human activity intensity. Inspired by the metaphor and analogy between the urban structure and topography, we developed an efficient method for identifying urban centers from the NPP-VIIRS NTL composite data. Our method has multiple advantages over the previous census-data-based methods.

First, our method detects not only the point location of urban centers but also their spatial extent and boundaries. Thus, it enables us to quantitatively analyze these urban centers' morphological properties and relevant indicators (e.g., NTL statistics). Moreover, the boundary of the detected urban center is not constrained by any preset census or other administrative units. Instead, it is precisely determined through the natural variation of NTL intensity at a pixel level. Second, this method is capable of determining urban centers' nested hierarchical spatial relationships, hence suitable for identifying composite centers or polycentric urban regions at different spatial scales. We can use composite urban centers, instead of just the elemental urban centers, to examine the urban spatial structure at a broader scale, such as intercity scale and transregional scale. In that case, the detected urban centers would represent highly urbanized regions or interlocked urban clusters. While this paper is focused on urban centers and subcenters' detection at intracity scale, it, in fact, provides essential information needed for examining the nested hierarchical structure of a complex, polycentric metropolitan area. Spatially, a complex metropolitan area is formed by nested urban areas and centers of varied scales. Our contour tree-based

analytical approach uncovers not only urban centers of different scales and their locations, but also urban areas at varied hierarchical levels and more importantly way in which urban centers or subcenters fit inside other broader, composite urban districts, and eventually the entire metropolitan area. The combination of the topological information about the nested hierarchical structure and the morphometric statistics provides comprehensive and essential knowledge for the classification of urban centers and urban districts across different scales in a metropolitan area. Third, by the analogy between the urban spatial structure and topography, more topographical features, such as "ridges," "valleys," "basins," can be introduced in detecting and interpreting urban morphological features from the NTL data. For example, a "ridge" in NTL data may indicate an urban development corridor. The introduction of more meaningful metaphors may help us acquire additional and valuable information about urban spatial structures.

It should be noted that the use of our method involves the selection of three parameters for processing the NPP-VIIRS NTL composite data. The selection of these parameters was mainly based on the trial-and-error experiments and local knowledge, and hence may be arbitrary and subjective to a certain extent. Additional techniques, such as machine learning, may be employed to derive an appropriate threshold value for detecting and locating urban centers when good training samples are available. Although empirical results presented in this study are specific to the case of Shanghai, the proposed method would be applicable to other regions owing to the global availability of the NPP-VIIRS NTL data and applicable algorithm. Four more applications have successfully been conducted to demonstrate how to extend the proposed urban center detection method to other world regions in the supporting document.

VI. CONCLUSION

The polycentric urban structure is becoming increasingly common in large metropolitan areas in the world. Studying the polycentric urban structure is helpful for understanding the urban development process and formulating better plans for the future urban growth. In this study, the NTL intensity measured by satellite sensors was conceptualized as a topography-like surface, reflecting the varying concentration levels of human activities. A mount with strong NTL intensity on the NTL surface indicates an urban center. By using the topography metaphor and NTL data, a localized contour tree method was developed to delimit urban centers and derive their attributes and spatial relationships at multiple spatial scales. In the case of Shanghai City, we have successfully identified 33 elemental urban centers, delineated their boundaries, determined the topological relationships between these centers, and revealed the hierarchical polycentric nature of the urban spatial structure. A polycentric urban form has clearly emerged in Shanghai. Most of the subcenters of Shanghai are so far distributed in the inner suburban areas within 30 km from the CBD, which may suggest that the suburbanization of Shanghai is still in early stage. The transformation from a monocentric structure to a polycentric structure involves strong imprints of the municipal government's planning and

development strategies, in clear contrast to the urban restructuring dominated by market forces in western cities. The “One City, Nine Towns Development Plan” and the “1-9-6-6” model have apparently laid out a polycentric blueprint for Shanghai’s future urban growth and restructuring.

Although functional, relational, and political dimensions of polycentricity are important in understanding the polycentric cities, the identification of multiple urban centers in physical form is the foundation for all further investigations. This research presents a new and efficient method for identifying urban centers and analyzing the morphological polycentricity in urban spatial structure. In comparison with the previous methods, our new method has multiple advantages, including the computational efficiency, the precise delineation of urban centers’ spatial extents, the derivation of multiple attributes for the detected urban centers, the determination of hierarchical spatial relationships between urban centers at different scales, and the applicability to other world regions. We believe that this new method would find various applications in such fields as urban morphology, urban land-use development, urban planning, urban policy evaluation, and beyond.

REFERENCES

- [1] E. W. Burgess, *The Growth of the City: An Introduction to a Research Project*. Chicago, IL, USA: Univ. Chicago Press, 1925.
- [2] H. Hoyt, *The Structure and Growth of Residential Neighborhoods in American Cities*. Washington, DC, USA: United States Government Printing Office, 1939.
- [3] C. D. Harris and E. L. Ullman, “The nature of cities,” *Ann. Amer. Acad. Political Social Sci.*, vol. 242, pp. 7–17, Sep. 1945.
- [4] S. Couturier *et al.*, “Morpho-spatial extraction of urban nuclei in diffusely urbanized metropolitan areas,” *Landscape Urban Planning*, vol. 101, no. 4, pp. 338–348, 2011.
- [5] H. Taubenböck, M. Wegmann, A. Roth, H. Mehl, and S. Dech, “Urbanization in India—Spatiotemporal analysis using remote sensing data,” *Comput. Environ. Urban Syst.*, vol. 33, no. 3, pp. 179–188, 2009.
- [6] J. Peng, S. Zhao, Y. Liu, and L. Tian, “Identifying the urban-rural fringe using wavelet transform and kernel density estimation: A case study in Beijing City, China,” *Environ. Model. Softw.*, vol. 83, pp. 286–302, Sep. 2016.
- [7] T. Tammaru, “Suburban growth and suburbanisation under central planning: The case of Soviet Estonia,” *Urban Stud.*, vol. 38, no. 8, pp. 1341–1357, 2001.
- [8] C. J. Mayer and C. T. Somerville, “Residential construction: Using the urban growth model to estimate housing supply,” *J. Urban Econ.*, vol. 48, no. 1, pp. 85–109, 2000.
- [9] N. Pfister, R. Freestone, and P. Murphy, “Polycentricity or dispersion?: Changes in center employment in metropolitan Sydney, 1981 to 1996,” *Urban Geogr.*, vol. 21, no. 5, pp. 428–442, 2000.
- [10] W. J. Coffey and R. G. Shearmur, “Agglomeration and dispersion of high-order service employment in the Montreal metropolitan region, 1981–96,” *Urban Stud.*, vol. 39, no. 3, pp. 359–378, 2002.
- [11] T. M. Stanback, Jr., *The New Suburbanization: Challenge to the Center City*. Boulder, CO, USA: Westview Press, 1991.
- [12] B. Sun *et al.*, “Test on the performance of polycentric spatial structure as a measure of congestion reduction in megacities: The case study of Shanghai,” *Urban Planning Forum*, vol. 207, no. 2, pp. 63–69, 2013.
- [13] P. Gaubatz, “China’s urban transformation: Patterns and processes of morphological change in Beijing, Shanghai and Guangzhou,” *Urban Stud.*, vol. 36, no. 9, pp. 1495–1521, 1999.
- [14] J. Feng, F. Wang, and Y. Zhou, “The spatial restructuring of population in metropolitan Beijing: Toward polycentricity in the post-reform era,” *Urban Geogr.*, vol. 30, no. 7, pp. 779–802, 2009.
- [15] L. Zhang, J. Peng, Y. Liu, and J. Wu, “Coupling ecosystem services supply and human ecological demand to identify landscape ecological security pattern: A case study in Beijing–Tianjin–Hebei region, China,” *Urban Ecosyst.*, vol. 20, no. 3, pp. 701–714, 2017.
- [16] X. Liu and M. Wang, “How polycentric is urban China and why? A case study of 318 cities,” *Landscape Urban Planning*, vol. 151, pp. 10–20, Jul. 2016.
- [17] G. Giuliano and K. A. Small, “Subcenters in the Los Angeles region,” *Regional Sci. Urban Econ.*, vol. 21, no. 2, pp. 163–182, 1991.
- [18] A. Anas, R. Arnott, and K. A. Small, “Urban spatial structure,” *J. Econ. Literature*, vol. 36, no. 3, pp. 1426–1464, Sep. 1998.
- [19] D. P. McMillen, “Identifying sub-centres using contiguity matrices,” *Urban Stud.*, vol. 40, no. 1, pp. 57–69, 2003.
- [20] R. Shearmur and W. J. Coffey, “A tale of four cities: Intrametropolitan employment distribution in Toronto, Montreal, Vancouver, and Ottawa–Hull, 1981–1996,” *Environ. Planning A*, vol. 34, no. 4, pp. 575–598, 2002.
- [21] K. A. Small and S. Song, “Population and employment densities: Structure and change,” *J. Urban Econ.*, vol. 36, no. 3, pp. 292–313, 1994.
- [22] S. Song, “Modelling worker residence distribution in the Los Angeles region,” *Urban Stud.*, vol. 31, no. 9, pp. 1533–1544, 1994.
- [23] J. F. McDonald, “The identification of urban employment subcenters,” *J. Urban Econ.*, vol. 21, no. 2, pp. 242–258, 1987.
- [24] J. F. McDonald and D. P. McMillen, “Employment subcenters and land values in a polycentric urban area: The case of Chicago,” *Environ. Planning A*, vol. 22, no. 12, pp. 1561–1574, 1990.
- [25] P. Gordon, H. W. Richardson, and H. L. Wong, “The distribution of population and employment in a polycentric city: The case of Los Angeles,” *Environ. Planning A*, vol. 18, no. 2, pp. 161–173, 1986.
- [26] D. P. McMillen, “Nonparametric employment subcenter identification,” *J. Urban Econ.*, vol. 50, no. 3, pp. 448–473, Nov. 2001.
- [27] C. L. Redfearn, “The topography of metropolitan employment: Identifying centers of employment in a polycentric urban area,” *J. Urban Econ.*, vol. 61, no. 3, pp. 519–541, May 2007.
- [28] J. F. McDonald and P. J. Prather, “Suburban employment centres: The case of Chicago,” *Urban Stud.*, vol. 31, no. 2, pp. 201–218, 1994.
- [29] J. R. Cladera, C. R. M. Duarte, and M. Moix, “Urban structure and polycentrism: Towards a redefinition of the sub-centre concept,” *Urban Stud.*, vol. 46, no. 13, pp. 2841–2868, 2009.
- [30] C. D. Elvidge *et al.*, “Relation between satellite observed visible-near infrared emissions, population, economic activity and electric power consumption,” *Int. J. Remote Sens.*, vol. 18, no. 6, pp. 1373–1379, Apr. 1997.
- [31] C. Lo, “Urban indicators of China from radiance-calibrated digital DMSP-OLS nighttime images,” *Ann. Assoc. Amer. Geogr.*, vol. 92, no. 2, pp. 225–240, 2002.
- [32] C. Small, F. Pozzi, and C. D. Elvidge, “Spatial analysis of global urban extent from DMSP-OLS night lights,” *Remote Sens. Environ.*, vol. 96, no. 3, pp. 277–291, 2005.
- [33] B. Yu *et al.*, “Object-based spatial cluster analysis of urban landscape pattern using nighttime light satellite images: A case study of China,” *Int. J. Geograph. Inf. Sci.*, vol. 28, no. 11, pp. 2328–2355, 2014.
- [34] H. Xu, H. Yang, X. Li, H. Jin, and D. Li, “Multi-scale measurement of regional inequality in Mainland China during 2005–2010 using DMSP/OLS night light imagery and population density grid data,” *Sustainability*, vol. 7, no. 10, p. 13469, 2015.
- [35] X. Li and D. Li, “Can night-time light images play a role in evaluating the Syrian Crisis?” *Int. J. Remote Sens.*, vol. 35, no. 18, pp. 6648–6661, 2014.
- [36] X. Li *et al.*, “Detecting 2014 Northern Iraq Insurgency using night-time light imagery,” *Int. J. Remote Sens.*, vol. 36, no. 13, pp. 3446–3458, 2015.
- [37] K. Shi *et al.*, “Urban expansion and agricultural land loss in China: A multiscale perspective,” *Sustainability*, vol. 8, no. 8, p. 790, 2016.
- [38] H. Letu, M. Hara, G. Tana, Y. Bao, and F. Nishio, “Generating the nighttime light of the human settlements by identifying periodic components from DMSP/OLS satellite imagery,” *Environ. Sci. Technol.*, vol. 49, no. 17, pp. 10503–10509, 2015.
- [39] M. M. Bennett and L. C. Smith, “Advances in using multitemporal night-time lights satellite imagery to detect, estimate, and monitor socioeconomic dynamics,” *Remote Sens. Environ.*, vol. 192, pp. 176–197, Apr. 2017.
- [40] K. Shi *et al.*, “Modeling spatiotemporal CO₂ (carbon dioxide) emission dynamics in China from DMSP-OLS nighttime stable light data using panel data analysis,” *Appl. Energy*, vol. 168, pp. 523–533, Apr. 2016.
- [41] H. Letu, T. Y. Nakajima, and F. Nishio, “Regional-scale estimation of electric power and power plant CO₂ emissions using defense meteorological satellite program operational linescan system nighttime satellite data,” *Environ. Sci. Technol. Lett.*, vol. 1, no. 5, pp. 259–265, May 2014.

- [42] H. Letu *et al.*, "Estimating energy consumption from nighttime DMPS/OLS imagery after correcting for saturation effects," *Int. J. Remote Sens.*, vol. 31, no. 16, pp. 4443–4458, Sep. 2010.
- [43] H. Letu, M. Hara, G. Tana, and F. Nishio, "A saturated light correction method for DMSP/OLS nighttime satellite imagery," *IEEE Trans. Geosci. Remote Sens.*, vol. 50, no. 2, pp. 389–396, Feb. 2012.
- [44] P. C. Sutton, "A scale-adjusted measure of 'Urban sprawl' using nighttime satellite imagery," *Remote Sens. Environ.*, vol. 86, no. 3, pp. 353–369, 2003.
- [45] L. Ma, J. Wu, W. Li, J. Peng, and H. Liu, "Evaluating saturation correction methods for DMSP/OLS nighttime light data: A case study from China's cities," *Remote Sens.*, vol. 6, no. 10, pp. 9853–9872, 2014.
- [46] S. D. Miller, S. P. Mills, C. D. Elvidge, D. T. Lindsey, T. F. Lee, and J. D. Hawkins, "Suomi satellite brings to light a unique frontier of nighttime environmental sensing capabilities," *Proc. Nat. Acad. Sci. USA*, vol. 109, no. 39, pp. 15706–15711, Sep. 2012.
- [47] K. Baugh, F.-C. Hsu, C. D. Elvidge, and M. Zhizhin, "Nighttime lights compositing using the VIIRS day-night band: Preliminary results," *Proc. Asia-Pacific Adv. Netw.*, vol. 35, pp. 70–86, Sep. 2013.
- [48] C. D. Elvidge, K. E. Baugh, M. Zhizhin, and F.-C. Hsu, "Why VIIRS data are superior to DMSP for mapping nighttime lights," *Proc. Asia-Pacific Adv. Netw.*, vol. 35, pp. 62–69, Apr. 2013.
- [49] C. D. Elvidge, M. Zhizhin, F.-C. Hsu, and K. Baugh, "What is so great about nighttime VIIRS data for the detection and characterization of combustion sources?" *Proc. Asia-Pacific Adv. Netw.*, vol. 35, pp. 33–48, Jun. 2013.
- [50] X. Li, H. Xu, X. Chen, and C. Li, "Potential of NPP-VIIRS nighttime light imagery for modeling the regional economy of China," *Remote Sens.*, vol. 5, no. 6, pp. 3057–3081, Jun. 2013.
- [51] K. Shi, C. Huang, B. Yu, B. Yin, Y. Huang, and J. Wu, "Evaluation of NPP-VIIRS night-time light composite data for extracting built-up urban areas," *Remote Sens. Lett.*, vol. 5, no. 4, pp. 358–366, Apr. 2014.
- [52] K. Shi *et al.*, "Evaluating the ability of NPP-VIIRS nighttime light data to estimate the gross domestic product and the electric power consumption of China at multiple scales: A comparison with DMSP-OLS data," *Remote Sens.*, vol. 6, no. 2, pp. 1705–1724, Feb. 2014.
- [53] T. Ma, C. Zhou, T. Pei, S. Haynie, and J. Fan, "Responses of Suomi-NPP VIIRS-derived nighttime lights to socioeconomic activity in China's cities," *Remote Sens. Lett.*, vol. 5, no. 2, pp. 165–174, Feb. 2014.
- [54] B. Yu, K. Shi, Y. Hu, C. Huang, Z. Chen, and J. Wu, "Poverty evaluation using NPP-VIIRS nighttime light composite data at the county level in China," *IEEE J. Sel. Topics Appl. Earth Observ. Remote Sens.*, vol. 8, no. 3, pp. 1217–1229, Mar. 2015.
- [55] Z. Chen, B. Yu, Y. Hu, C. Huang, K. Shi, and J. Wu, "Estimating house vacancy rate in metropolitan areas using NPP-VIIRS nighttime light composite data," *IEEE J. Sel. Topics Appl. Earth Observ. Remote Sens.*, vol. 8, no. 5, pp. 2188–2197, May 2015.
- [56] Q. Wu, H. Liu, S. Wang, B. Yu, R. Beck, and K. Hinkel, "A localized contour tree method for deriving geometric and topological properties of complex surface depressions based on high-resolution topographical data," *Int. J. Geograph. Inf. Sci.*, vol. 29, no. 12, pp. 2041–2060, 2015.
- [57] X. Jiangang, L. Banggu, S. Qing, Z. Feng, and M. Anxin, "Urban spatial restructuring in transitional economy—Changing land use pattern in Shanghai," *Chin. Geograph. Sci.*, vol. 17, no. 1, pp. 19–27, Apr. 2007.
- [58] Y. Sha, J. Wu, Y. Ji, S. Li, T. Chan, and W. Q. Lim, "Evolution of urban planning and city development of Shanghai: The past three eras and the present," in *Shanghai Urbanism at Medium Scale*. Berlin, Germany: Springer, 2014, pp. 9–18.
- [59] W. Yue, P. Fan, and J. Qi, "Spatio-temporal evolution of urban structure in Shanghai," in *Vulnerability of Land Systems in Asia*. Chichester, U.K.: Wiley, 2014, p. 215.
- [60] J. He, "Implementation of the Shanghai master plan (2001–2020)," in *Proc. 26th Annu. Congr. (AESOP) (METU)*, Ankara, Turkey, 2012, pp. 1–22.
- [61] H. Pan, "Shanghai from dense mono-center to organic poly-center urban expansion," in *Proc. Better Air Quality Meet.*, Yogyakarta, Indonesia, 2006, pp. 1–22.
- [62] B. Sun, W. Shi, and Y. Ning, "An empirical study on the polycentric urban structure of shanghai and strategies in future," *Urban Planning Forum*, vol. 23, no. 1, pp. 58–63, 2010.
- [63] Y. Shi, "From a singe center city to a multi-centers city—Spatial organization pattern of metropolitan development in China," *Urban Planning Rev.*, vol. 3, p. 008, Sep. 1999.
- [64] N. Levin, "The impact of seasonal changes on observed nighttime brightness from 2014 to 2015 monthly VIIRS DNB composites," *Remote Sens. Environ.*, vol. 193, pp. 150–164, May 2017.
- [65] C. D. Elvidge *et al.*, "VIIRS nightfire: Satellite pyrometry at night," *Remote Sens.*, vol. 5, no. 9, pp. 4423–4449, 2013.
- [66] N. Levin and Q. Zhang, "A global analysis of factors controlling VIIRS nighttime light levels from densely populated areas," *Remote Sens. Environ.*, vol. 190, pp. 366–382, Sep. 2017.
- [67] A. C. Nelson, "Using land markets to evaluate urban containment programs," *J. Amer. Planning Assoc.*, vol. 52, no. 2, pp. 156–171, 1986.
- [68] P. A. Burrough and R. A. McDonnell, *Principles of Geographical Information Systems*. Oxford, U.K.: Oxford Univ. Press, 2011.
- [69] L. B. Liao, S. Weiss, S. Mills, and B. Hauss, "Suomi NPP VIIRS day-night band on-orbit performance," *J. Geophys. Res.-Atmos.*, vol. 118, no. 22, pp. 12705–12718, Nov. 2013.
- [70] Q. Wu and C. R. Lane, "Delineation and quantification of wetland depressions in the Prairie Pothole Region of North Dakota," *Wetlands*, vol. 36, no. 2, pp. 215–227, 2016.
- [71] I. S. Kweon and T. Kanade, "Extracting topographic terrain features from elevation maps," *Image Understand.*, vol. 59, no. 2, pp. 171–182, 1994.
- [72] H. Liu, L. Wang, D. Sherman, Y. Gao, and Q. Wu, "An object-based conceptual framework and computational method for representing and analyzing coastal morphological changes," *Int. J. Geograph. Inf. Sci.*, vol. 24, no. 7, pp. 1015–1041, Jul. 2010.
- [73] J. C. Davis and R. J. Sampson, *Statistics and Data Analysis in Geology*. New York, NY, USA: Wiley, 1986.
- [74] N. Green, "Functional polycentricity: A formal definition in terms of social network analysis," *Urban Stud.*, vol. 44, no. 11, pp. 2077–2103, 2007.
- [75] X. Liu, B. Derudder, and K. Wu, "Measuring polycentric urban development in China: An intercity transportation network perspective," *Regional Stud.*, vol. 50, no. 8, pp. 1–14, 2015.
- [76] C. O. Tong and S. C. Wong, "The advantages of a high density, mixed land use, linear urban development," *Transportation*, vol. 24, no. 3, pp. 295–307, 1997.
- [77] C. He *et al.*, "Restoring urbanization process in China in the 1990s by using non-radiance-calibrated DMSP/OLS nighttime light imagery and statistical data," *Chin. Sci. Bull.*, vol. 51, no. 13, pp. 1614–1620, 2006.
- [78] Y. Zhou *et al.*, "A global map of urban extent from nightlights," *Environ. Res. Lett.*, vol. 10, no. 5, p. 054011, 2015.



Zuqi Chen received the B.S. degree in cartography and geographic information system from Fujian Normal University, Fuzhou, China, in 2011, and the Ph.D. degree from East China Normal University, Shanghai, China, in 2017.

He is currently a Post-Doctoral Fellow with the Key Laboratory of Geographic Information Science, Ministry of Education, East China Normal University, Shanghai, where he is also with the School of Geographic Sciences. His research interests include urban remote sensing, nighttime light remote sensing, and the development of GIS.



Bailang Yu (M'09–SM'17) received the B.S. and Ph.D. degrees in cartography and geographic information systems from East China Normal University, Shanghai, China, in 2002 and 2009, respectively.

He is currently a Professor with the Key Laboratory of Geographic Information Science, Ministry of Education, East China Normal University, Shanghai, where he is also with the School of Geographic Sciences. His research interests include urban remote sensing, nighttime light remote sensing, LiDAR, and object-based methods.



Wei Song received the B.S. degree in economic geography from Peking University, Beijing, China, and the Ph.D. degree in location analysis and GIS from The Ohio State University, Columbus, OH, USA.

He is currently an Associate Professor with the Department of Geography and Geosciences, University of Louisville, Louisville, KY, USA, where he is also a Ph.D. Faculty Member of urban and public affairs and an Affiliated Faculty Member of Asian studies. His research interests include urban geography, location and transportation analysis, quantitative methods, and applications of Geographic Information System (GIS).



Hongxing Liu (M'00) received the Ph.D. degree in geography from The Ohio State University, Columbus, OH, USA, in 1999.

His recent research projects have been funded by NASA, NSF, and NOAA Sea Grant Program. His research interests include remote sensing, geographical information science, hydrological modeling, terrain analysis, coastal mapping, and change studies.

Dr. Liu received a number of prestigious awards, including the NASA Group Achievement Award, the Best Paper Award from Computers & Geoscience, and the Distinguished Achievement Award for Teaching from the College of Geoscience at Texas A&M University.



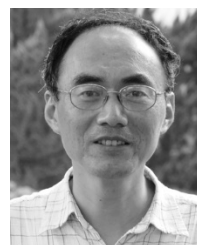
Kaifang Shi received the M.S. degree in physical geography from Southwest University, Chongqing, China, in 2013, and the Ph.D. degree in cartography and geographic information systems from East China Normal University, Shanghai, China, in 2017.

His research interests include the application of GIS, remote sensing application in socioeconomic characterization and urbanization process, and land-use planning.



Qiusheng Wu received the Ph.D. degree in geography from the University of Cincinnati, Cincinnati, OH, USA.

He is currently an Assistant Professor with the Department of Geography, Binghamton University, State University of New York, Binghamton, NY, USA. His research interests include LiDAR remote sensing, GIS, terrain analysis, and wetland hydrology.



Jianping Wu received the M.S. degree from Peking University, Beijing, China, in 1986, and the Ph.D. degree from East China Normal University, Shanghai, China, in 1996.

He is currently a Professor with East China Normal University. His research interests include remote sensing and geographic information system.